



Universiteit
Leiden
The Netherlands

Growing oxide thin films in a low-energy electron microscope

Torren, A.J.H. van der

Citation

Torren, A. J. H. van der. (2016, December 5). *Growing oxide thin films in a low-energy electron microscope*. *Casimir PhD Series*. Retrieved from <https://hdl.handle.net/1887/44732>

Version: Not Applicable (or Unknown)

License: [Licence agreement concerning inclusion of doctoral thesis in the Institutional Repository of the University of Leiden](#)

Downloaded from: <https://hdl.handle.net/1887/44732>

Note: To cite this publication please use the final published version (if applicable).

Cover Page



Universiteit Leiden



The handle <http://hdl.handle.net/1887/44732> holds various files of this Leiden University dissertation

Author: Torren, Alexander J.H. van der

Title: Growing oxide thin films in a low-energy electron microscope

Issue Date: 2016-12-05

2

The $\text{LaAlO}_3/\text{SrTiO}_3$ interface

LaAlO₃ and SrTiO₃ are cubic perovskites and wide band gap insulators which differ in one aspect: SrTiO₃ is a non-polar material, where each layer stacked along a principal axis of the cube is charge-neutral. LaAlO₃ is polar, with layers having alternating charges of $\pm e$ per unit cell. In 2004, Ohtomo and Wang made the remarkable discovery of a two dimensional electron gas (2-DEG) forming at the interface. Such a conducting layer has potential for applications, but despite much research, many details of its formation are still unclear. This chapter describes the basic understanding of the LaAlO₃/SrTiO₃ interface.

2.1 Transition-metal oxides

Transition metal oxides (TMO's) show many exciting phenomena compared to simple covalent semiconductors. Strong Coulomb repulsion between the 3d electrons of the TM ion, parametrized by U , tend to localize them on the atoms, leading to an insulating state. The energy gap to the conducting states is roughly determined by $U - 2zt$, where t is the site-to-site transfer integral of the d-electrons, and z is the number of nearest neighbors. If $t \ll U$, as is often the case, this leads to the so-called Mott-insulating state. Such an insulator is very different from covalent semiconductors such as Si, and GaAs, where the four hybridized sp^3 electrons form shared pairs with four nearest neighbor atoms. The electrons localize between the atoms, as a result of the competition between electron-nucleus attraction and electron-electron repulsion. The Mott state is charge-ordered, but the subtle interplay between charge, spin, and lattice structure also leads to spin and orbital order. Figure 2.1a and b show the doping phase diagrams of $\text{La}_{1-x}\text{Sr}_x\text{MnO}_3$ and

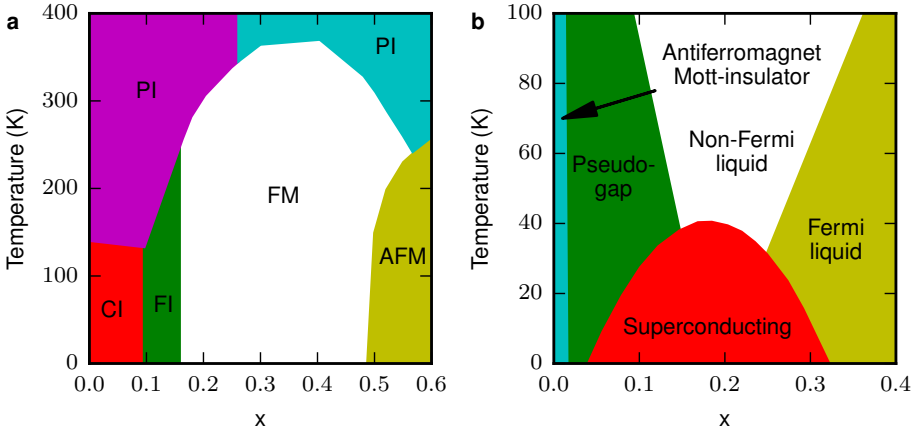


FIGURE 2.1: Phase diagram of (a) $\text{La}_{1-x}\text{Sr}_x\text{MnO}_3$, based on data from Ref. ¹⁻³. PM, PI, FM, AFM, FI, and CI denote, paramagnetic metal, paramagnetic insulator, ferromagnetic metal, antiferromagnetic metal, ferromagnetic insulator, and spin-canted insulator states, respectively. (b) $\text{La}_{2-x}\text{Sr}_x\text{CuO}_4$, based on data from Ref. ⁴.

$\text{La}_{2-x}\text{Sr}_x\text{CuO}_4$, respectively. In $(\text{La},\text{Sr})\text{MnO}_3$ the Sr^{2+} ion dopes holes into the MnO_2 complex, leading to a mix of Mn^{3+} and Mn^{4+} valencies. The latter results in a hole in the d-band and (at low temperatures) a change from an antiferromagnetic canted insulator (CI in Fig. 2.1a) to a ferromagnetic metal (FM). This state becomes paramagnetic insulating at higher temperatures, resulting in the well-known colossal magnetoresistance effect. In $(\text{La},\text{Sr}_2)\text{CuO}_4$ the doping leads to even more dramatic effects. Doping holes into the CuO_2 complexes now yields high-temperature superconductivity.

The effective masses of charge carriers in TMOs are an order of magnitude higher than in semiconductors, which is partly due to the strong coupling with the lattice and the reorientation possibilities for the oxygen octahedra. Together with high carrier concentrations this leads to short screening lengths for electric fields, in the order of 1 to 100 nm.

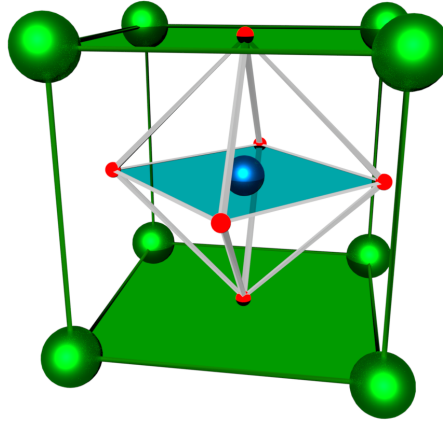


FIGURE 2.2: Unit cells of the perovskite structure with the ABO_3 chemical formula. Here A is in green (corner), B in blue (center) and O in red (cube faces). Furthermore, the AO plane is shown in green and the BO_2 plane in blue.

A much studied structure of TMOs is the cubic perovskite structure (Fig. 2.2). The chemical structure is ABO_3 . Here the A is an alkaline earth metal or a rare earth metal and the B is a transition metal or a metalloid. Under pressure and temperature the structure can change from cubic to orthorhombic, tetragonal, rhombohedral or monoclinic. Along the (001) direction the structure can be seen as, built up from AO and BO_2 planes, indicated with blue and green planes in figure 2.2.

In this thesis I will focus on the 2-dimensional electron gas between the TMOs $SrTiO_3$ and $LaAlO_3$. Strictly speaking, $SrTiO_3$ is a TMO, but not a Mott-insulator, the Ti^{4+} has an empty d-shell. However, doping can fill the Ti d-shell in the $SrTiO_3$, showing TMO physics. Moreover, $LaAlO_3$ is not strictly a TMO, since Al is not a transition metal, but structure and physics is close to the one of the TMOs and it is in general seen as part of the group. $SrTiO_3$ and $LaAlO_3$ are both perovskites and insulators with bandgaps of 3.2 eV⁵ and 5.6 eV⁶ respectively. Their lattice constants (STO : 3.905 Å⁷, LAO : 3.789 Å⁸) have only a small mismatch of 3 %, resulting in epitaxial growth when stacking the two materials. Both materials are widely used as substrates, and are easily commercially available as single crystals. As-received crystals have a mixed terminated surface with both areas with AO and BO_2 planes. For $SrTiO_3$ the termination can chemically be changed to TiO_2 ^{9,10}, whereas the SrO termination can only be made reliably by growing a monolayer of

SrO on a TiO_2 terminated surface. For LaAlO_3 the termination is more complex and it will be discussed in chapter 4.

2.2 The $\text{LaAlO}_3/\text{SrTiO}_3$ Interface

At the interface of LaAlO_3 and SrTiO_3 a conducting interface is found. This is a different interface than in covalent semiconductors. Where for instance at the

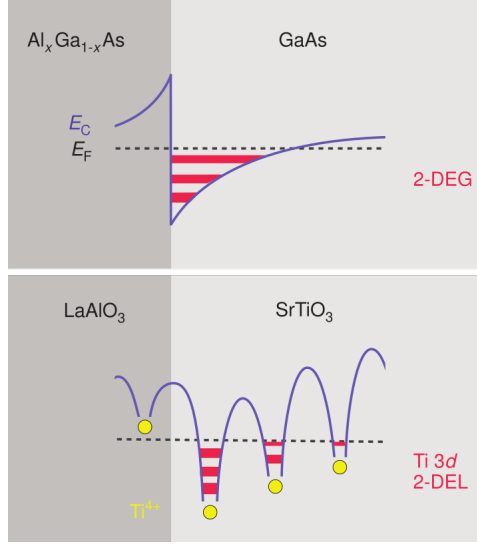


FIGURE 2.3: Comparison between the 2-DEG at the $\text{GaAs}/\text{Al}_x\text{Ga}_{1-x}\text{As}$ interface (top) and the 2-DEL at the $\text{LaAlO}_3/\text{SrTiO}_3$ interface (bottom). Taken from Ref. ¹¹.

interface of the covalent semiconductors $\text{GaAs}/\text{Al}_x\text{Ga}_{1-x}\text{As}$ the mobile carriers move into two-dimensional subbands within the quantum well generated by band bending, at the $\text{LaAlO}_3/\text{SrTiO}_3$ interface multiple quantum wells are found given by the ionic potentials of the TiO_6 octahedra (see fig. 2.3). The electrons are subject to the correlations of the Ti 3d bands and form an two dimensional electron liquid (2-DEL) rather than a gas¹². This electron liquid is strongly confined, which is very advantageous for screening and switching applications as well as for miniaturization of devices. For historic reasons we will often still use 2-DEG instead of 2-DEL.

The interface can actually be made in two different configurations. First, when the SrTiO_3 is TiO_2 terminated, growing epitaxial LaAlO_3 results in a TiO_2/LaO interface, which can become conducting. Second, when the terminating layer is SrO the interface will be SrO/AlO_2 . This interface turns out to be insulating^{13,14}. For the conducting interface, Thiel *et al.*¹⁵ found that the surface only becomes conducting when the LaAlO_3 layer consists of four or more unit cells. One and two unit cells result in a fully insulating interface, while a three-unit-cell interface can be made conducting by gating.

2.2. The $\text{LaAlO}_3/\text{SrTiO}_3$ Interface

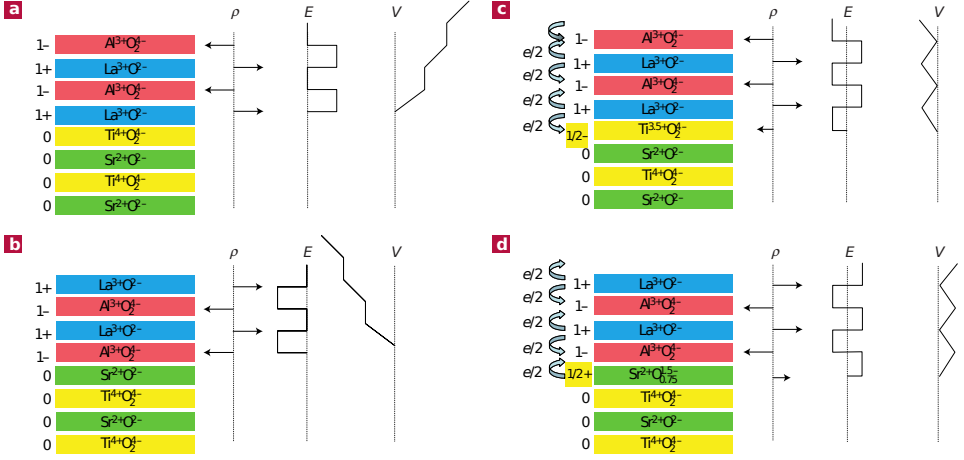


FIGURE 2.4: Illustration of the polar catastrophe model in the $\text{LaAlO}_3/\text{SrTiO}_3$ hetero-structure. The stacking sequence of LaAlO_3 and SrTiO_3 layers is shown with their oxidation levels and final net charge per layer. In the diagrams ρ is the net charge per layer, E the resulting electric field and V the potential buildup. a and b illustrate the potential buildup for a n-type (TiO_2/LaO) and p-type (SrO/AlO_2) interface respectively, leading to a diverging potential. In c half an electron charge is transferred from the surface to the interface to avoid the divergence. For the p-type interface, one would expect the electron is transferred from the interface to the surface. However, an energetically more favorable structural reconstruction¹⁶ appears. Image from Ref. 14.

To understand this remarkable effect of a 2-dimensional electron gas between two insulators, the role of the SrTiO_3 and LaAlO_3 layers are now further discussed. These building blocks can be described as stacked AO and BO_2 layers as stated earlier. Writing down these layers and their charges we find for the SrTiO_3 , $\text{Sr}^{2+}\text{O}^{2-}$ and $\text{Ti}^{4+}\text{O}_2^-$, both having zero net charge. In contrast, for LaAlO_3 the layers are $\text{La}^{3+}\text{O}^{2-}$ and $\text{Al}^{3+}\text{O}_2^-$, respectively positive and negatively charged. This is illustrated in figure 2.4. The charged layers in the LaAlO_3 can be seen as parallel plate capacitors with a charge ρ , resulting in an electric field E between them, which results in a potential buildup V . Starting from a neutral SrTiO_3 layer the potential builds up without bound, as the thickness of LaAlO_3 grows (Fig. 2.4a), which is not physically possible. This can be solved by an electronic or structural reconstruction. In the case of an electronic reconstruction, half an electron is transferred from the LaAlO_3 surface towards the interface (Fig. 2.4c), resulting in half a free electron per unit cell at the interface creating half the charge at the interface. This is the so called polar catastrophe^{13,14} model. This potential buildup fits reasonably well with the transition from insulating to conducting interface at three to four unit cells. Only for four unit cells and more the potential buildup is strong enough for the electron transfer to take place.

The resulting electrons at the interface will change the Ti^{4+} to Ti^{3+} . In that case, we call it a n-type interface. On the other hand if the SrTiO_3 surface is SrO terminated the potential buildup is opposite (Fig. 2.4b) and half an electron has

to be transferred away from the interface to the LaAlO_3 surface (Fig. 2.4d). This would result in a p-type interface as an electron has to be removed from the O-2p band. This is energetically more expensive and a structural reconstruction is more favorable¹⁶ resulting in an insulating interface.

Although this model presents a good description of the conducting interface, it cannot be the full story. In particular core-level X-ray photoemission spectroscopy (XPS) measurements have not been able to measure the potential buildup^{17,18}. Furthermore, there is strong evidence for an important role of defects and stoichiometry, which now will be discussed.

2.3 Oxygen vacancies

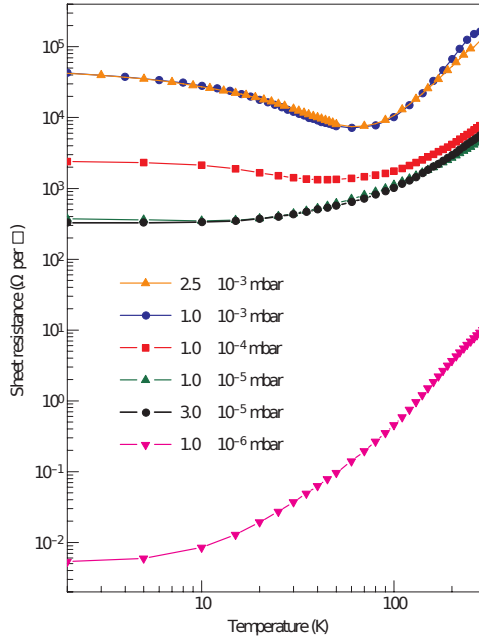


FIGURE 2.5: Sheet resistance as function of temperature of the $\text{LaAlO}_3/\text{SrTiO}_3$ interface depending on oxygen background pressure during growth as indicated in the figure. Note the minimum who occurs for pressures above 10^{-4} mbar. Taken from Ref.¹⁹.

The number of oxygen vacancies is mainly influenced by the oxygen background pressure during growth and is well described by Brinkman *et al.*¹⁹. Figure 2.5 summarizes the salient behavior of the sheet resistance of the interface as function of temperature for different values of the oxygen background pressure during growth. At pressures of 1×10^{-6} mbar and lower the amount of oxygen in the SrTiO_3 crystal is reduced and bulk conductivity starts to play a role. For pressures above 1×10^{-2} mbar the interface is found the be insulating, while in the intermediate

regime different types of physics are found at the interface, such as superconductivity^{20–22} and magnetism^{19,23–25}. The minimum occurring at pressures above 1×10^{-4} mbar is often connected to the presence of some kind of magnetism. To stay clearly away from bulk conductivity, but preserve UHV conditions in our low-energy electron microscope without taking extra precautions, we decided to use a background pressure of 5×10^{-5} mbar O_2 in the experiments involving the $LaAlO_3/SrTiO_3$ interface.

2.4 Stoichiometry

It has been found that also the stoichiometry of the deposited $LaAlO_3$ -layer is of crucial importance for rendering the interface conducting or insulating^{26–29}. Warusawithana *et al.*²⁷ using molecular beam epitaxy (MBE), found that the La/Al ratio has to be smaller than 0.97 to obtain a conducting interface. Breckenfeld *et al.*³⁰, using PLD, found that at 2 K the interface sheet resistances using 4 % La-deficient $LaAlO_3$ is almost ten orders of magnitude lower than the interface sheet resistance using 5 % La-excess $LaAlO_3$. Also, Dildar *et al.*²⁶ found that $LaAlO_3$ deposited on $SrTiO_3$ by sputtering in 1 mbar of oxygen showed a La-excess of 7 %, while the interface was insulating. This stoichiometry dependence emphasizes the importance of defects in the $SrTiO_3$ and $LaAlO_3$ during the formation of the interface conductance. In particular, it has been pointed out that excess Al can substitute on the La-sites, while La excess leads to Al_2O_3 -vacancy complexes²⁷, with significant differences in the way the charge distribution problem can be solved. However, how this exactly leads to either a conducting or a non-conducting interface is not yet fully understood.

The stoichiometry issue is the more important since it is strongly influenced by the growth conditions. Growth of $LaAlO_3/SrTiO_3$ interfaces is most frequently performed by pulsed laser deposition (PLD), the primary work horse for complex oxide growth. Apart from the fact that PLD is a relative cheap option compared to MBE, it was long believed that PLD was a technique which would transfer a material preserving the stoichiometry. However, also PLD is a complex process where laser fluence and background pressure play an important role in the stoichiometry of the film. Here the ablation efficiency of the ions and the scattering processes between ions and the background gas play an important role³¹. In these scattering processes the particle mass is very important, changing the stoichiometry of the plume. All in all, having some knowledge of the stoichiometry during growth, also in deposition processes where the elements are not controlled separately as in MBE, would be quite advantageous. We shall come back to this issue in chapter 6.

References

- [1] E. Dagotto, T. Hotta, and A. Moreo, *Colossal magnetoresistant materials: the key role of phase separation*, Physics Reports **344**, 1 (2001).
- [2] A. Urushibara, Y. Moritomo, T. Arima, A. Asamitsu, G. Kido, and Y. Tokura, *Insulator-metal transition and giant magnetoresistance in $\text{La}_{1-x}\text{Sr}_x\text{MnO}_3$* , Physical Review B **51**, 14103 (1995).
- [3] H. Fujishiro, M. Ikebe, and Y. Konno, *Phase Transition to Antiferromagnetic State in $\text{La}_{1-x}\text{Sr}_x\text{MnO}_3$ ($x \approx 0.5$)*, Journal of the Physical Society of Japan **67**, 1799 (1998).
- [4] M. P. M. Dean, G. Dellea, R. S. Springell, F. Yakhou-Harris, K. Kummer, N. B. Brookes, X. Liu, Y.-J. Sun, J. Strle, T. Schmitt, L. Braicovich, G. Ghiringhelli, I. Boovi, and J. P. Hill, *Persistence of magnetic excitations in $\text{La}_{2x}\text{Sr}_x\text{CuO}_4$ from the undoped insulator to the heavily overdoped non-superconducting metal*, Nature Materials **12**, 1019 (2013).
- [5] H. Weakliem, W. Burke, and V. Korsun, *Optical Properties of SrTiO_3 and LiNbO_3* , R.C.A. Review **36**, 149 (1975).
- [6] S.-G. Lim, S. Kriventsov, T. N. Jackson, J. H. Haeni, D. G. Schlom, A. M. Balbashov, R. Uecker, P. Reiche, J. L. Freeouf, and G. Lucovsky, *Dielectric functions and optical bandgaps of high- K dielectrics for metal-oxide-semiconductor field-effect transistors by far ultraviolet spectroscopic ellipsometry*, Journal of Applied Physics **91**, 4500 (2002).
- [7] J. G. Bednorz and H. J. Scheel, *Flame-fusion growth of SrTiO_3* , Journal of Crystal Growth **41**, 5 (1977).
- [8] S. Geller and V. B. Bala, *Crystallographic studies of perovskite-like compounds. II. Rare earth alluminates*, Acta Crystallographica **9**, 1019 (1956).
- [9] M. Kawasaki, K. Takahashi, T. Maeda, R. Tsuchiya, M. Shinohara, O. Ishiyama, T. Yonezawa, M. Yoshimoto, and H. Koinuma, *Atomic Control of the SrTiO_3 Crystal Surface*, Science **266**, 1540 (1994).
- [10] G. Koster, B. L. Kropman, G. J. H. M. Rijnders, D. H. A. Blank, and H. Rogalla, *Quasi-ideal strontium titanate crystal surfaces through formation of strontium hydroxide*, Applied Physics Letters **73**, 2920 (1998).
- [11] J. Mannhart and D. G. Schlom, *Oxide Interfaces—An Opportunity for Electronics*, Science **327**, 1607 (2010).
- [12] M. Breitschaft, V. Tinkl, N. Pavlenko, S. Paetel, C. Richter, J. R. Kirtley, Y. C. Liao, G. Hammerl, V. Eyert, T. Kopp, and J. Mannhart, *Two-dimensional electron liquid state at $\text{LaAlO}_3\text{-SrTiO}_3$ interfaces*, Physical Review B **81**, 153414 (2010).

- [13] A. Ohtomo and H. Y. Hwang, *A high-mobility electron gas at the $\text{LaAlO}_3/\text{SrTiO}_3$ heterointerface*, Nature **427**, 423 (2004).
- [14] N. Nakagawa, H. Y. Hwang, and D. A. Muller, *Why some interfaces cannot be sharp*, Nature Materials **5**, 204 (2006).
- [15] S. Thiel, G. Hammerl, A. Schmehl, C. W. Schneider, and J. Mannhart, *Tunable Quasi-Two-Dimensional Electron Gases in Oxide Heterostructures*, Science **313**, 1942 (2006).
- [16] L. Zhang, X.-F. Zhou, H.-T. Wang, J.-J. Xu, J. Li, E. G. Wang, and S.-H. Wei, *Origin of insulating behavior of the p-type $\text{LaAlO}_3/\text{SrTiO}_3$ interface: Polarization-induced asymmetric distribution of oxygen vacancies*, Physical Review B **82**, 125412 (2010).
- [17] Y. Segal, J. H. Ngai, J. W. Reiner, F. J. Walker, and C. H. Ahn, *X-ray photoemission studies of the metal-insulator transition in $\text{LaAlO}_3/\text{SrTiO}_3$ structures grown by molecular beam epitaxy*, Physical Review B **80**, 241107 (2009).
- [18] M. Takizawa, S. Tsuda, T. Susaki, H. Y. Hwang, and A. Fujimori, *Electronic charges and electric potential at $\text{LaAlO}_3/\text{SrTiO}_3$ interfaces studied by core-level photoemission spectroscopy*, Physical Review B **84**, 245124 (2011).
- [19] A. Brinkman, M. Huijben, M. van Zalk, J. Huijben, U. Zeitler, J. C. Maan, W. G. van der Wiel, G. Rijnders, D. H. A. Blank, and H. Hilgenkamp, *Magnetic effects at the interface between non-magnetic oxides*, Nature Materials **6**, 493 (2007).
- [20] N. Reyren, S. Thiel, A. D. Caviglia, L. F. Kourkoutis, G. Hammerl, C. Richter, C. W. Schneider, T. Kopp, A.-S. Ruetschi, D. Jaccard, M. Gabay, D. A. Muller, J.-M. Triscone, and J. Mannhart, *Superconducting Interfaces Between Insulating Oxides*, Science **317**, 1196 (2007).
- [21] A. Joshua, S. Pecker, J. Ruhman, E. Altman, and S. Ilani, *A universal critical density underlying the physics of electrons at the $\text{LaAlO}_3/\text{SrTiO}_3$ interface*, Nature Communications **3**, 1129 (2012).
- [22] A. D. Caviglia, S. Gariglio, N. Reyren, D. Jaccard, T. Schneider, M. Gabay, S. Thiel, G. Hammerl, J. Mannhart, and J.-M. Triscone, *Electric field control of the $\text{LaAlO}_3/\text{SrTiO}_3$ interface ground state*, Nature **456**, 624 (2008).
- [23] Ariando, X. Wang, G. Baskaran, Z. Q. Liu, J. Huijben, J. B. Yi, A. Annadi, A. R. Barman, A. Rusydi, S. Dhar, Y. P. Feng, J. Ding, H. Hilgenkamp, and T. Venkatesan, *Electronic phase separation at the $\text{LaAlO}_3/\text{SrTiO}_3$ interface*, Nature Communications **2**, 188 (2011).
- [24] D. A. Dikin, M. Mehta, C. W. Bark, C. M. Folkman, C. B. Eom, and V. Chandrasekhar, *Coexistence of Superconductivity and Ferromagnetism in Two Dimensions*, Physical Review Letters **107**, 056802 (2011).

- [25] J. A. Bert, B. Kalisky, C. Bell, M. Kim, Y. Hikita, H. Y. Hwang, and K. A. Moler, *Direct imaging of the coexistence of ferromagnetism and superconductivity at the $\text{LaAlO}_3/\text{SrTiO}_3$ interface*, Nature Physics **7**, 767 (2011).
- [26] I. M. Dildar, D. B. Boltje, M. H. S. Hesselberth, J. Aarts, Q. Xu, H. W. Zandbergen, and S. Harkema, *Non-conducting interfaces of $\text{LaAlO}_3/\text{SrTiO}_3$ produced in sputter deposition: The role of stoichiometry*, Applied Physics Letters **102**, 121601 (2013).
- [27] M. P. Warusawithana, C. Richter, J. A. Mundy, P. Roy, J. Ludwig, S. Paetel, T. Heeg, A. A. Pawlicki, L. F. Kourkoutis, M. Zheng, M. Lee, B. Mulcahy, W. Zander, Y. Zhu, J. Schubert, J. N. Eckstein, D. A. Muller, C. S. Hellberg, J. Mannhart, and D. G. Schlom, *LaAlO_3 stoichiometry is key to electron liquid formation at $\text{LaAlO}_3/\text{SrTiO}_3$ interfaces*, Nature Communications **4** (2013).
- [28] H. K. Sato, C. Bell, Y. Hikita, and H. Y. Hwang, *Stoichiometry control of the electronic properties of the $\text{LaAlO}_3/\text{SrTiO}_3$ heterointerface*, Applied Physics Letters **102**, 251602 (2013).
- [29] E. Breckenfeld, R. Wilson, J. Karthik, A. R. Damodaran, D. G. Cahill, and L. W. Martin, *Effect of Growth Induced (Non)Stoichiometry on the Structure, Dielectric Response, and Thermal Conductivity of SrTiO_3 Thin Films*, Chemistry of Materials **24**, 331 (2012).
- [30] E. Breckenfeld, N. Bronn, J. Karthik, A. R. Damodaran, S. Lee, N. Mason, and L. W. Martin, *Effect of Growth Induced (Non)Stoichiometry on Interfacial Conductance in $\text{LaAlO}_3/\text{SrTiO}_3$* , Physical Review Letters **110**, 196804 (2013).
- [31] S. Wicklein, A. Sambri, S. Amoruso, X. Wang, R. Bruzzese, A. Koehl, and R. Dittmann, *Pulsed laser ablation of complex oxides: The role of congruent ablation and preferential scattering for the film stoichiometry*, Applied Physics Letters **101**, 131601 (2012).